Theoretical and Experimental Studies of Ducted Mixing and Burning of Coaxial Streams

C. E. Peters,* W. J. Phares,† and T. H. M. Cunningham‡
ARO Inc., Arnold Air Force Station, Tenn.

An extensive investigation of the ducted turbulent mixing process is described. Experimental results are presented for a rocket-air mixing system which is typical of the air-augmented rocket. An integral theory for the duct flow is presented, for arbitrary axisymmetric duct geometry and for either frozen or equilibrium mixing zone chemistry. The turbulent shear stress in the variable density mixing layer is treated by use of a modified Prandtl eddy viscosity model. The outer (secondary) inviscid portion of the flow is treated as one-dimensional. The central (primary) inviscid stream is treated with a coupled method of characteristics solution for supersonic primary streams. Comparison of the theory with experiments indicates that the theory is applicable to engineering analysis of ducted mixing systems, such as air-air ejectors and air-augmented rockets.

Nomenclature

AAR = air-augmented rocket
b = mixing zone width
B = determinant in equation for db/dx
C_k = mass fraction of element k
$\bar{C}$ = mass fraction of elements from central stream
D = coefficient determinant for system of equations
$F_1 \ldots F_4$ = coefficients in system of differential equations
F_d = mixing duct thrust
F_n = vacuum thrust of primary nozzle
$G_1 \ldots G_4$ = coefficients in system of differential equations
H_0 = total, or stagnation, enthalpy, including chemical heats of formation
$H_1 \ldots H_4$ = coefficients in system of differential equations
$J_1 \ldots J_4$ = general coefficients [Eq. (12)]
k = constant in eddy viscosity equation
k_0 = incompressible eddy viscosity constant
L = length of mixing duct
M = Mach number
p = static pressure
p_b = back pressure
p_0 = total, or stagnation, pressure
P = determinant in equation for dp_w/dx
Q = species conservation parameter
r = radial coordinate
r_n = radius of primary nozzle exit
R = determinant in equation for dr_i/dx
S_{1g}, S_{2g} = general integrands (Appendix)
T_0 = total, or stagnation, temperature
u = axial velocity component
u_{max}, u_{min} = maximum and minimum velocities in mixing layer
v = transverse or radial velocity component
V = magnitude of total velocity vector
w_a = initial mass flow of secondary stream
w_j = initial mass flow of primary stream
x = axial coordinate
ϵ = turbulent eddy viscosity
θ = flow angle
ρ = density
τ = turbulent shear stress

Subscripts

1 = mixing duct inlet
a = inviscid secondary flow
c = centerline
g = index of differentiation (Appendix)
i = inner mixing zone boundary
j = primary stream
m = half-radius control surface in mixing zone
w = duct wall

Presented as Paper 69-85 at the AIAA 7th Aerospace Sciences Meeting, New York, January 20–22, 1969; submitted January 31, 1969; revision received September 29, 1969. This research was sponsored by the Arnold Engineering Development Center (AEDC), Air Force Systems Command, under Contract F40600-69-C-0001 with ARO Inc. Further reproduction is authorized to satisfy the needs of the U.S. Government.

* Supervisor of Fluid Dynamics and Propulsion Section, Research Branch, Rocket Test Facility. Member AIAA.
† Analyst, Central Computer Operations.
‡ Research Engineer, Rocket Test Facility; now with AiResearch Manufacturing Company, Phoenix, Ariz. Member AIAA.

Introduction

DUCTED turbulent mixing of coaxial streams occurs in many devices of practical interest to the engineer. Typical examples are the jet pump (or air-air ejector) and composite propulsion systems such as the air-augmented rocket (AAR).[1,2] An extensive theoretical and experimental investigation of ducted mixing has been in progress at the Rocket Test Facility of AEDC for several years.[3–5] The basic objective of this research has been to develop an adequate engineering theory to describe the ducted mixing process, including chemical reactions, which is encountered in the AAR and other composite propulsion systems. Emphasis has been placed on relatively long mixing systems in which the duct pressure distribution is strongly influenced by thick mixing layers. In other words, this may be considered a strong viscous interaction problem.

The mixing system is shown schematically in Fig. 1. The specific objective is to predict the secondary mass flow w_a and the duct wall pressure distribution if the following parameters are prescribed: 1) geometry, 2) primary (jet) fluid and initial conditions, 3) secondary fluid and stagnation conditions, p_{0a}

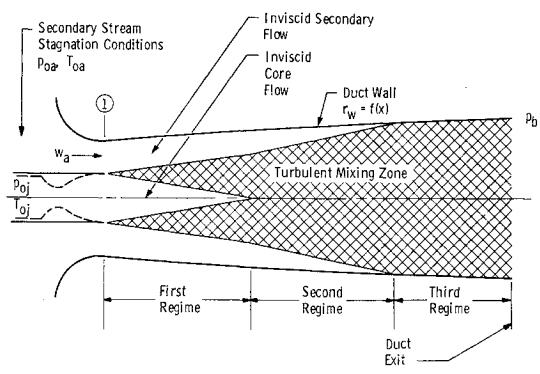

Fig. 1 Schematic of ducted mixing system.

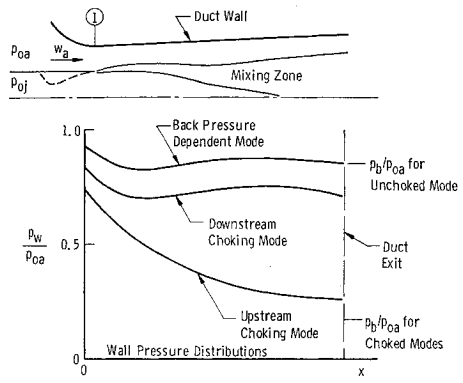

Fig. 2 Operational modes of a ducted mixing system.

and T_{0a}, and 4) back pressure, p_b. Three distinct flow regimes are shown in Fig. 1: 1) turbulent mixing between the secondary flow and the inviscid primary flow, 2) continued mixing after the inviscid core has been dissipated, but a region of inviscid secondary flow exists near the duct wall, and 3) entirely turbulent flow.

Three modes of operation are possible for a ducted mixing system when the primary stream is initially supersonic and the secondary stream is initially subsonic (Fig. 2). These modes are distinguished by the factor which limits the secondary mass flow rate, w_a. The "upstream choking" mode occurs when w_a is limited by choking of the secondary flow near the entrance of the duct. The primary stream has expanded, causing the secondary flow area at the choke point to be less than the initial flow area. Fabri and Paulon[6] called this mode the "supersonic regime." The "downstream choking" mode occurs when w_a is limited by choking of the flow at the duct exit. This mode may occur even in a divergent mixing duct if the fluids have greatly different densities or exothermic chemical reactions occur, and it is of interest for AAR's.[4] The "back pressure dependent" mode occurs when p_b is sufficiently high to unchoke the duct flow. The secondary flow is subsonic throughout the duct, and the duct exit pressure exactly matches the back pressure. Fabri called this mode the "mixed regime." It is commonly encountered in jet pumps but is not of practical interest for AAR's.

To be considered adequate, a generalized theory for the ducted mixing system must be capable of predicting both the operational mode and the resulting performance. Two analytical models have been developed during this investigation.[5] In the first model, the inviscid portions of the primary and secondary flows are assumed to be one-dimensional (1-D Core Theory). The inviscid and viscous portions of the flow are computed simultaneously, and all three regimes in Fig. 1 are treated by use of the von Kármán integral method. This model may be considered an extension and refinement of the theory reported earlier.[3] It is satisfactory for subsonic mixing systems but not for supersonic primary flows, particularly when operating in the upstream choking mode. Consequently, the theory in the first regime was modified to include computation of the inviscid core flow with the irrotational method of characteristics. In the resulting "2-D Core Theory" model, the second and third regime treatment is the same as in the 1-D Core Theory.

The 1-D Core Theory has been correlated with a variety of subsonic mixing experiments,[5] both to establish the validity of the theory and to define the eddy viscosity constants for subsonic flows. Because the main emphasis of this work has been placed on mixing systems with supersonic primary streams, only the 2-D Core Theory will be described in this paper.

Other investigators have developed analytical models for treating the ducted mixing problem, including the influence of chemical reactions in the mixing layer. Edelman and Fortune[7] have developed an analytical model which is similar in many respects to the 1-D Core Theory, except that the viscous layer is computed with finite difference methods rather than with the integral method. Edelman and Fortune can compute mixing solutions with finite rate chemistry, whereas the present analysis is limited to equilibrium chemistry. Their analytical model is not applicable to ducted mixing systems with nonuniform supersonic primary flows. More recently, Edelman and Weilerstein[8] have developed an analysis for the fully supersonic ducted mixing process; their analysis is not applicable to the case of supersonic primary flow and subsonic secondary flow.

To the authors' knowledge, the 2-D Core Theory of the present investigation is the first successful attempt to couple, in a noniterative manner, the boundary-layer-type solution of the viscous layer with the method of characteristics solution of the supersonic inviscid core. The work most closely related to the 2-D Core Theory is that of Chow and Addy[9] on the supersonic air-air ejector operating in the upstream choking mode. The supersonic air-air ejector represents a weak viscous interaction problem because viscous effects are small except at low and zero secondary flow rates. In the analysis of Chow and Addy, the primary stream is computed with the method of characteristics and the inviscid secondary flow is computed simultaneously by use of the one-dimensional assumption. The inviscid solution is then corrected for viscous effects along the jet boundary separating the primary and secondary fluids. The Chow and Addy theory[9] is applicable to nonconstant area mixing ducts[10] (such as short thrust augmentation devices, e.g., turbojet ejector nozzles). Mixing systems with thick mixing layers cannot be analyzed with the Chow and Addy technique of superposition of a two-dimensional mixing layer onto the inviscid jet boundary.

Because of the many simplifications required in any analysis of ducted turbulent mixing, it is essential that the validity of the theoretical models be established by detailed comparisons with experiment in the flow regime of interest. Consequently, extensive experiments have been made at AEDC on a ducted rocket-air mixing system which is representative of the air-augmented rocket.[3,4] The rocket-air mixing system was operated in all of the modes shown in Fig. 2.

Theoretical Analysis—2-D Core Theory

The principal assumptions are:

1) The flow is axisymmetric.

2) All gases obey the perfect gas law.

3) The usual boundary-layer assumptions are applicable to the mixing layer.

4) The inviscid portion of the secondary flow is one-dimensional and isentropic.

5) The inviscid portion of the primary flow is isentropic.

6) The mixing layer is fully turbulent and boundary layers at initiation of mixing are negligible.

7) Viscous effects at the duct wall are negligible (the no-slip condition is not applied at the wall).

8) The mixing zone velocity profiles are assumed to have similar shapes (cosine function).

9) The turbulent Prandtl and Lewis numbers are unity.

10) For mixing with simultaneous chemical reactions, the reactions are assumed to be in equilibrium.

11) In the third regime (Fig. 1), the free mixing concepts of shear and profile shape similiarity are assumed to be applicable.

For mathematical convenience, the viscous effects are considered only in the mixing layer which is assumed to have discrete boundaries. By integrating the continuity and boundary-layer momentum equations, we obtain three basic integral equations (Fig. 3): 1) a continuity equation for the flow between r_i and r_w, 2) a momentum equation for the flow between r_i and r_w, and 3) a momentum equation for the flow between r_i and a control surface r_m, arbitrarily located halfway across the mixing layer.

Continuity Equation

$$\frac{d}{dx}\int_{ri}^{rw} \rho u r dr = \rho_i v_i r_i - \rho_i u_i r_i \frac{dr_i}{dx} \quad (1)$$

Momentum Equation

$$\frac{d}{dx}\int_{ri}^{rw} \rho u^2 r dr = \rho_i u_i v_i r_i - \rho_i u_i^2 r_i \frac{dr_i}{dx} - \frac{dp_w}{dx}\left[\frac{r_w^2 - r_i^2}{2}\right] \quad (2)$$

Half-Radius Momentum Equation

$$\frac{d}{dx}\int_{ri}^{rm} \rho u^2 r dr - u_m \frac{d}{dx}\int_{ri}^{rm} \rho u r dr = (u_m - u_i)\left(\rho_i u_i r_i \frac{dr_i}{dx} - \rho_i v_i r_i\right) + \tau_m r_m - \frac{dp_w}{dx}\left[\frac{r_m^2 - r_i^2}{2}\right] \quad (3)$$

The term τ_m in Eq. (3) represents the turbulent shear stress at the half-radius control surface. In the second and third regimes, $r_i = 0$, and the integral equations are considerably simplified. The isobaric axisymmetric boundary-layer equations for momentum, energy, and conservation of elemental species have been given by Libby[11] for unity turbulent Prandtl and Lewis numbers. These three equations have the same form for the variables, u, H_0, and C_k, and the following linear relations are obtained between these variables for negligible initial boundary layers:

$$\frac{u - u_a}{u_i - u_a} = \frac{H_0 - H_{0a}}{H_{0i} - H_{0a}} = \frac{C_k - C_{ka}}{C_{ki} - C_{ka}} \quad (4)$$

The subscripts a and i refer to the inviscid conditions at either edge of the mixing layer. Because the transport coefficients for all species are the same, the composition at any point in the mixing zone may be characterized as a simple two-component mixture. Thus,

$$\frac{u - u_a}{u_i - u_a} = \frac{H_0 - H_{0a}}{H_{0i} - H_{0a}} = \bar{C} \quad (4a)$$

where $\bar{C}$ is the local mass fraction of elements from the central stream.

Although derived for isobaric flow, Eq. (4a) is conditionally assumed to be valid for flows with axial pressure gradients. It should be noted, however, that the inviscid reference velocities, u_i and u_a, are pressure dependent and will vary in a typical ducted mixing problem. If Eq. (4a) is valid, then the computed total flux of elements from the central stream should be the same at all axial stations. In other words, the solution of the integrated momentum equation is also a satisfactory solution for the integrated species and energy equations.

A species conservation parameter Q may be defined as

$$Q = \left(\frac{2\pi}{w_j}\right)\int_0^{rw} \rho u \bar{C} r dr \quad (5)$$

It has been found that Q does remain approximately unity throughout typical air-augmented rocket systems.[5] Therefore, the use of Eq. (4a) is justified, at least from an integral point of view, for such systems.

Mixing Zone Profiles and Eddy Viscosity

The mixing zone velocity profiles are represented by a cosine function:

$$\frac{u - u_{\min}}{u_{\max} - u_{\min}} = \frac{1}{2} + \frac{1}{2}\cos\left[\pi\frac{(r - r_i)}{b}\right] \quad (6)$$

In the first and second regimes (Fig. 3), $u_{\min} = u_a$; in the third regime, $u_{\min} = u_w$. In the first regime, $u_{\max} = u_i$; in the second and third regimes, $u_{\max} = u_c$.

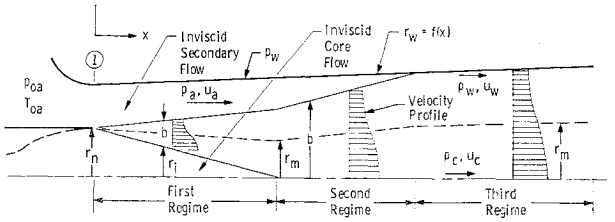

Fig. 3 Nomenclature for integral analysis.

In the first regime, u_i is defined as

$$u_i = V_i \cos\theta_i \quad (7)$$

where V_i is the magnitude of the total velocity vector at r_i (an isentropic function of p_w) and θ_i is the flow angle at r_i.

At the half-radius control surface,

$$u_m = \tfrac{1}{2}(u_{\max} + u_{\min}) \quad (8)$$

For rocket-air mixing, the mixing zone compositions and temperatures are determined by an approximate equilibrium chemistry computation.[5] The density is thus determined as a function of p_w and the local velocity in the mixing layer.

Turbulent Eddy Viscosity

The term τ_m in Eq. (3) is determined by

$$\tau_m = \rho_m \epsilon_m \partial u/\partial r|_m \quad (9)$$

where ϵ_m is the turbulent eddy viscosity. The model for the eddy viscosity which is used in this work is the incompressible Prandtl model,

$$\epsilon = kb(u_{\max} - u_{\min}) \quad (10)$$

with the empirical constant k corrected for the effect of variable density. The correction used is a modification of the technique suggested by Donaldson and Gray.[12] Donaldson and Gray found that the influence of variable density could be generalized if k is taken to be a function of the local mach number, M_m, at the half-radius control surface. The following empirical equation was developed during this investigation[5] to express the relation between k and the incompressible constant, k_0:

$$k/k_0 = 0.66 + 0.34\exp(-3.42\,M_m^2) \quad (11)$$

The 1-D Core Theory has been correlated with low speed air-air mixing experiments, and it was found that $k_0 = 0.007$ in the first regime, and $k_0 = 0.011$ in the second and third regimes. These values have been used for all of the computations presented in this paper and in Ref. 5.

It should be noted that the Prandtl eddy viscosity model [Eq. (10)] is known to be deficient when u_a/u_i exceeds about 0.3. Also, Eq. (11) has not been checked against a sufficient number of experiments to be considered completely reliable. Nevertheless, the present eddy viscosity model gave good results for the AEDC experimental rocket-air mixing configurations.[3,4] In those experiments, u_a/u_i did not exceed 0.1.

Transformation of Integral Equations

Sufficient information is available so that the terms in Eqs. (1–3) can be related to three flowfield variables. In the first regime (Fig. 3), these variables are selected to be p_w, r_i, and b. In the second regime, the selected variables are p_w, u_c, and b. In the third regime, the selected variables are p_w, u_c, and u_w.

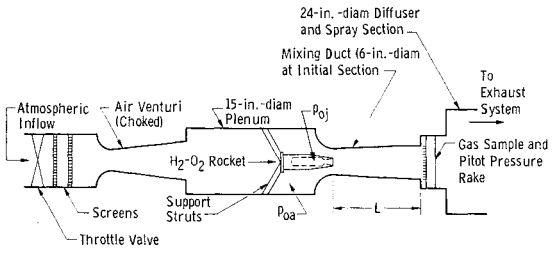

Fig. 4 Schematic of experimental apparatus.

In the first regime, Eqs. (1–3) can be transformed into the following system:

$$J_1 \frac{dp_w}{dx} + J_2 \frac{dr_i}{dx} + J_3 \frac{db}{dx} = J_4 \tag{12}$$

where $J \equiv F$ for the continuity equation, $J \equiv G$ for the momentum equation, and $J \equiv H$ for the half-radius momentum equation. The equations for the coefficients are presented in the Appendix. The numerous auxiliary equations necessary for computation of the coefficients have been presented in Ref. 5.

Equations (12) can be solved for the derivatives (dp_w/dx, dr_i/dx, and db/dx) by use of Cramer's rule, as long as the determinant of the coefficients is not zero;

$$\frac{dp_w}{dx} = \frac{P}{D}, \quad \frac{dr_i}{dx} = \frac{R}{D}, \quad \frac{db}{dx} = \frac{B}{D} \tag{13}$$

The D, P, R, and B represent coefficient determinants for the preceding system of differential equations. Equations (13) are numerically integrated by use of the well-known Runge-Kutta method. An IBM 360/50 computer was used to obtain the numerical solutions.

The transformation in the second and third regimes is similar to the first regime except that the derivatives in question are (dp_w/dx, du_c/dx, db/dx) and (dp_w/dx, du_c/dx, du_w/dx), respectively.[5]

Method of Solution

Many terms appearing in the first regime coefficients (F, G, and H) depend on the flow conditions at the inner mixing zone boundary. In order to solve the system of differential equations, one must be able to evaluate the following properties at r_i: θ_i, $\partial u/\partial x$, $\partial u/\partial r$, $\partial p/\partial x$, and $\partial p/\partial r$. To provide these parameters, the inviscid core flow is computed (with the irrotational method of characteristics) simultaneously with the numerical solution of the equations for the mixing layer and inviscid secondary flow.[5] The key technique used to couple the solution of the viscous layer with the solution of the inviscid core flow is as follows. At each intermediate Runge-Kutta step in the numerical integration of Eqs. (13), the method of characteristics is used to solve for the flow conditions at r_i (θ_i, etc.). All of the inner boundary derivatives also are defined, and the coefficients (F, G, and H) can be evaluated. By using this technique, the entire flowfield is solved in a stepwise manner in the axial direction.

The solution for the ducted mixing system is obtained by iteration of the initial static pressure, p_{w1}, until some downstream boundary condition is satisfied.[5] In the back pressure dependent mode of operation (Fig. 2), the boundary condition is to match the computed wall pressure at the duct exit with the prescribed back pressure, p_b. In the downstream choking mode (Fig. 2), the boundary condition is that the determinant D of the system of equations must be zero at the duct exit. Therefore, $D = 0$ is considered to correspond to physical choking.

The solution technique is more complex for mixing systems operating in the upstream chocking mode (Fig. 2). The initial static pressure, p_{w1}, is iterated until the determinants D and P are simultaneously zero, as required for dp_w/dx to be bounded. The determinants R and B are also zero at the critical section. The solution then proceeds downstream into the supercritical region.

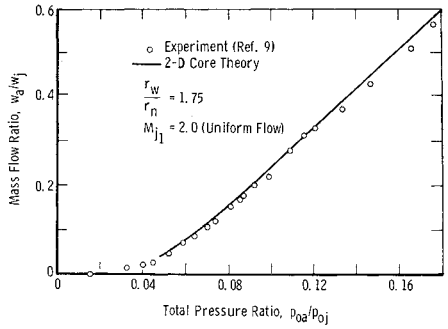

Fig. 5 Mass flow ratio for a cylindrical air-air ejector.

Ducted Rocket-Air Mixing Experiments

The apparatus shown in Fig. 4 was installed in Propulsion Research Cell (R-1B) of the Rocket Test Facility. The primary stream was provided by a hydrogen-oxygen rocket operated at approximately 2.5 times the stoichiometric fuel flow. Gaseous propellants were used to obtain a high combustion efficiency. The average characteristic velocity was greater than 96% of the ideal value for 51 rocket firings. The secondary flow was room temperature air at subatmospheric total pressure. Major dimensions of the apparatus and typical operating parameters are given in Table 1.

Experimental data are presented[3,4] for two mixing duct configurations: a conical duct (2.98° half-angle) with $L = 5.17$ r_{w1} and the basic conical duct with a cylindrical extension added ($L = 7.17\ r_{w1}$). In addition to the pressures, temperatures, and flow rates of the secondary air and rocket propellants, measurements were made of 1) wall pressure distribution along the mixing duct and 2) radial distributions of pitot pressure and gas composition at the exit plane of the mixing duct. With the exhaust pressure at the desired value, the desired secondary flow was set by adjusting the throttle valve located upstream from the choked metering nozzle. The rocket was then fired for a nominal duration of 30 sec. The system was allowed to stabilize for 20 sec before gas samples were collected and pressures were recorded.

Comparison of Theory and Experiment

Supersonic Air-Air Ejectors

The 2-D Core Theory has been correlated[5] with the air ejector experiments of Chow and Addy[9] and of Chow and Yeh.[10] Only the constant area configuration of Chow and Addy, which operated in the upstream choking mode, will be considered here.

The experimental mass flow ratios are shown in Fig. 5, along with the results of the 2-D Core Theory. The agreement between theory and experiment is very satisfactory for

Table 1 Major dimensions of apparatus and typical operating parameters

Rocket chamber pressure, p_{oj}	300 psia
Rocket mixture ratio, by mass	3.15
Total rocket mass flow, w_j	0.98 lbm/sec
Rocket nozzle:	
Throat diameter	1.00 in.
Expansion cone half angle	15°
Expansion area ratio	5.25
Inlet radius of mixing duct, r_{w1}	3 in.
Nozzle exit radius/duct inlet radius, r_n/r_{w1}	0.38

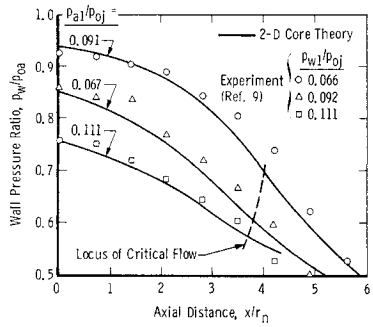

Fig. 6 Wall pressure distributions in a cylindrical air-air ejector.

the entire range of p_{0a}/p_{0j} over which the theory is applicable. No attempt was made in this investigation to extend the 2-D Core Theory to the case of zero and very low secondary flows. The theoretical results of Chow and Addy are not shown in Fig. 5; their results are nearly identical to the 2-D Core Theory results.

The experimental and theoretical wall pressure distributions for the constant area air-air ejector are shown in Fig. 6. It should be noted that the critical flow does not correspond to $M_a = 1$, except when the computations are made with zero mixing rate. The secondary stream Mach number is always subsonic at the critical ($D = 0$) section for finite mixing rates. The 2-D Core Theory also gives very satisfactory correlation[5] of the experimental performance of the nonconstant area ejector configurations of Chow and Yeh.

AEDC Ducted Rocket-Air Experiments

Upstream choking mode

The basic conical mixing duct was operated in the upstream choking mode.[3] A typical experimental wall pressure distribution is shown in Fig. 7, along with the theoretical results for no mixing and for mixing with equilibrium chemistry. The theory shows that the inviscid pressure distribution is significantly altered by mixing and combustion, especially in the downstream portion of the duct. The theoretical pressure distribution (with equilibrium chemistry) predicts the experimental pressure distribution reasonably well. The differences between theory and experiment are attributed to shock waves in the supersonic portion of the flow; these shock waves are neglected in the theory. Only the first mixing regime was encountered in this configuration. The theory predicts secondary-primary mass flow ratios which are 4–5% higher than the experimental ratios (Fig. 8).

In any propulsion system application, an important parameter is the mixing duct thrust F_d, defined by

$$F_d = 2\pi \int_0^L p_w r_w \left(\frac{dr_w}{dx}\right) dx$$

where L is the length of the mixing duct. The ratio of F_d to the vacuum thrust of the rocket, F_n, is shown in Fig. 8. The

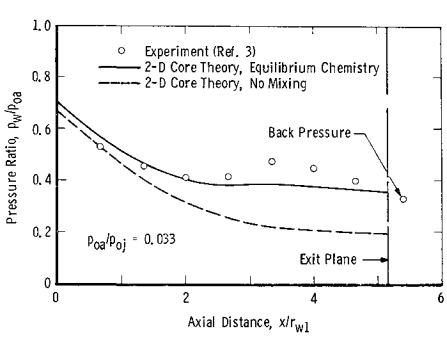

Fig. 7 Wall pressure distribution for ducted rocket-air mixing (upstream choking mode).

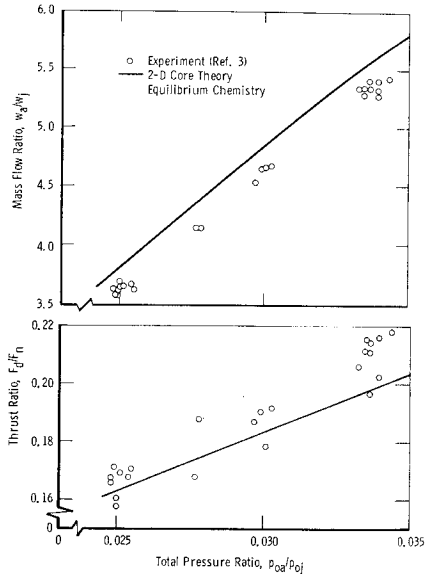

Fig. 8 Mass flow ratio and mixing duct thrust for rocket-air mixing (upstream choking mode).

theory predicts a thrust ratio which agrees with experiment to within 10% over the range of p_{0a}/p_{0j} considered.

Downstream choking mode

The conical mixing duct with cylindrical extension was operated in the downstream choking mode.[4] A typical wall pressure distribution is shown in Fig. 9, along with the theoretical result for equilibrium mixing zone chemistry. The theoretical wall pressures are higher than the experimental pressures, but the shape of the experimental pressure distribution is correctly predicted. As was the case with the upstream choking mode results, the differences between theory and experiment are attributed to shock waves in the primary flow. It should be noted that the inviscid core flow is completely dissipated in this configuration, and the flow at the duct exit is in the second mixing regime. The theoretical secondary-primary mass flow ratios are 10 to 15% higher than the experimental ratios (Fig. 10). The theoretical thrust ratio (Fig. 10) is approximately 6% larger than experiment at the lower values of p_{0a}/p_{0j} and approximately 16% too large at the higher values of p_{0a}/p_{0j}.

Comparison of upstream and downstream choking modes

The inviscid solutions for the conical duct and the conical duct with cylindrical extension are identical. Both inviscid systems operate in the upstream choking mode, and at a given value of p_{0a}/p_{0j}, both systems have the same w_a and the same F_d. The solutions which include mixing, however, show that the longer duct operates in the downstream choking mode, and

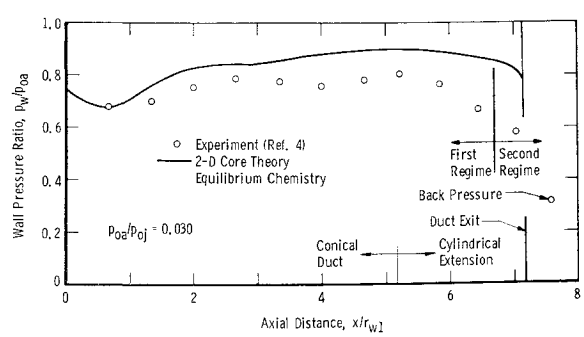

Fig. 9 Wall pressure distribution for ducted rocket-air mixing (downstream choking mode).

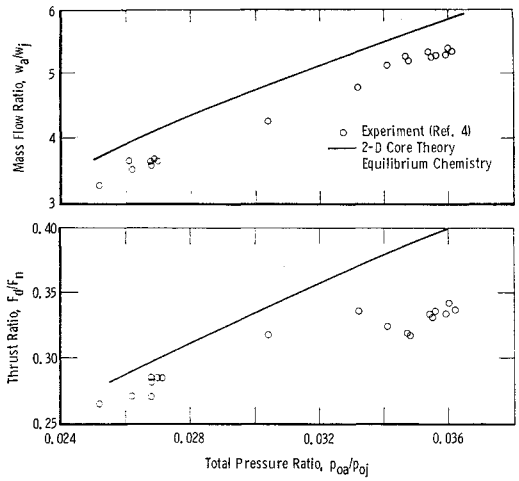

Fig. 10 Mass flow ratio and mixing duct thrust for rocket-air mixing (downstream choking mode).

that the mixing has caused the entire character of the flow to change from the inviscid character. The solutions show that the shorter duct operates in the upsteam choking mode, either with or without mixing. As a result, the theoretical values of w_a and F_d (with mixing) are considerably different for the two ducts.

A comparison of Figs. 8 and 10 shows that the experimental secondary mass flow was decreased by approximately 10% with the addition of the cylindrical extension. The experimental mixing duct thrust (Figs. 8 and 10) was increased by 50–60%. These comparisons show the desirability of the downstream choking mode for the AAR. The mixing duct thrust F_d represents the gross thrust increase for the augmentation duct; the net thrust comparison (F_d minus inlet and external drag) is even more favorable for operation in the downstream choking mode.

Back pressure dependent mode

The conical mixing duct with cylindrical extension was operated in the back pressure dependent mode.[4] These results are not of primary interest for the AAR and are not presented here. In general, the 2-D Core Theory satisfactorily predicts the mixing duct thrust, but the predicted secondary mass flow is too large. Again, this difference between theory and experiment is attributed to the presence shock waves in the primary flow.

Duct exit plane profiles

Radial distributions of Pitot pressure and gas composition were measured at the duct exit plane during the AEDC experiments. The 2-D Core Theory satisfactorily predicts the experimental Pitot pressures profiles over the outer part of the mixing zone, but the experimental Pitot pressures are lower than the theoretical pressures near the duct centerline.[5] The low Pitot pressures near the duct centerline are caused by strong shock waves in the inviscid core flow; these shocks are neglected in the theory.

The gas composition profiles were obtained by sampling. Dry mole fraction distributions of H_2, N_2, and O_2 are shown in Fig. 11 for one test condition using the conical duct with cylindrical extension. Figure 11 is a composite plot of data from several rocket firings at the same nominal test condition, and the data were obtained on both sides of the duct centerline. The theory predicts the experimental profiles very well, indicating that the assumption of equilibrium chemistry is valid for this mixing configuration. The width of the mixing zone is also correctly predicted, indicating that the eddy viscosity model used in the theory is satisfactory for this mixing system.

Concluding Remarks

An extensive theoretical and experimental investigation of ducted mixing of coaxial streams has been summarized. Experimental results have been presented for a rocket-air mixing system typical of the air-augmented rocket. An analytical model has been presented which includes the effects of 1) a nonuniform supersonic core flow and 2) equilibrium chemical reactions in the mixing layer. Even though the current detailed knowledge about turbulent flows with chemical reactions is meager, the use of integral methods permits reasonably accurate computations of the flow in complex mixing systems.

The analytical and experimental results which have been presented show that the viscous effects are predominant in certain types of ducted mixing systems. Consequently, it is essential that the viscous and inviscid portions of the flow be computed simultaneously for such mixing systems.

The main emphasis of this work has been placed on mixing systems which are strongly influenced by the mixing process. Of course, the theoretical model is also applicable to flows which are weakly influenced by mixing, such as supersonic air-air ejectors, but the theory offers no quantitative improvement over the superposition technique of Chow and Addy.

The weakest aspect of the present theory is the assumption that the inviscid core flow is shock-free. Also, the eddy viscosity model used cannot be considered reliable except for mixing systems with small secondary-primary velocity ratios.

Although the theoretical model has several deficiencies, the results are qualitatively correct. In addition, the theoretical results are sufficiently accurate so that the theory may be considered useful for engineering analysis of ducted mixing systems.

Appendix

The following parameters are defined:

$$y = (r - r_i)/b$$

$$S_{1g} = \rho \frac{\partial u}{\partial g} + u \frac{\partial \rho}{\partial g} \text{ where } g = p_w, r_i, b, \text{ and } x$$

$$S_{2g} = 2\rho u \frac{\partial u}{\partial g} + u^2 \frac{\partial \rho}{\partial g}$$

The first regime coefficients (F, G, and H) are

$$F_1 = b^2 \int_0^1 S_{1p_w} y dy + br_i \int_0^1 S_{1p_w} dy + \tfrac{1}{2}[r_w^2 - (r_i + b)^2] \left[\rho_a \frac{du_a}{dp_w} + u_a \frac{d\rho_a}{dp_w}\right]$$

$$F_2 = b^2 \int_0^1 S_{1r_i} y dy + br_i \int_0^1 S_{1r_i} dy$$

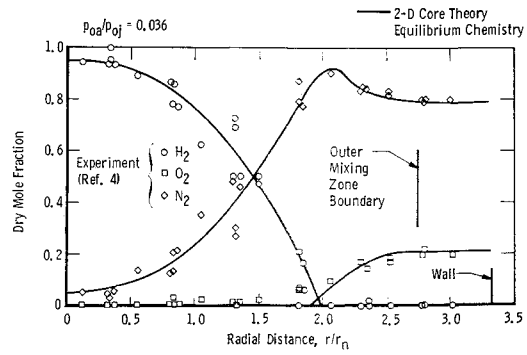

Fig. 11 Exit plane composition profiles for ducted rocket-air mixing (downstream choking mode).

$$F_3 = b^2 \int_0^1 S_{1b} y dy + br_i \int_0^1 S_{1b} dy$$

$$F_4 = -b^2 \int_0^1 S_{1x} y dy - br_i \int_0^1 S_{1x} dy + \rho_i v_i r_i - \rho_a u_a r_w \frac{dr_w}{dx}$$

$$G_1 = b^2 \int_0^1 S_{2p_w} y dy + br_i \int_0^1 S_{2p_w} d_y + \tfrac{1}{2} [r_w^2 - r_i^2] \left[1 + 2\rho_a u_a \frac{du_a}{dp_w} + u_a{}^2 \frac{d\rho_a}{dp_w}\right]$$

$$G_2 = b^2 \int_0^1 S_{2r_i} y dy + br_i \int_0^1 S_{2r_i} dy$$

$$G_3 = b^2 \int_0^1 S_{2b} y dy + br_i \int_0^1 S_{2b} dy$$

$$G_4 = -b^2 \int_0^1 S_{2x} y dy - br_i \int_0^1 S_{2x} dy + \rho_i u_i v_i r_i - \rho_a u_a{}^2 r_w \frac{dr_w}{dx}$$

$$H_1 = b^2 \int_0^{\frac{1}{2}} S_{2p_w} y dy + br_i \int_0^{\frac{1}{2}} S_{2p_w} dy - u_m b^2 \int_0^{\frac{1}{2}} S_{1p_w} y dy - u_m br_i \int_0^{\frac{1}{2}} S_{1p_w} dy + \frac{1}{2}\left[\left(r_i + \frac{b}{2}\right)^2 - r_i^2\right]$$

$$H_2 = b^2 \int_0^{\frac{1}{2}} S_{2r_i} y dy + br_i \int_0^{\frac{1}{2}} S_{2r_i} dy - u_m b^2 \int_0^{\frac{1}{2}} S_{1r_i} y dy - u_m br_i \int_0^{\frac{1}{2}} S_{1r_i} dy$$

$$H_3 = b^2 \int_0^{\frac{1}{2}} S_{2b} y dy + br_i \int_0^{\frac{1}{2}} S_{2b} dy - u_m b^2 \int_0^{\frac{1}{2}} S_{1b} y dy - u_m br_i \int_0^{\frac{1}{2}} S_{1b} dy$$

$$H_4 = -b^2 \int_0^{\frac{1}{2}} S_{2x} y dy - br_i \int_0^{\frac{1}{2}} S_{2x} dy + u_m b^2 \int_0^{\frac{1}{2}} S_{1x} y dy + u_m br_i \int_0^{\frac{1}{2}} S_{1x} dy + (u_i - u_m)\rho_i v_i r_i + \tau_m \left(r_i + \frac{b}{2}\right)$$

References

[1] Perini, L. et al., "Preliminary Study of Air Augmentation of Rocket Thrust," *Journal of Spacecraft and Rockets*, Vol. 1, No. 6, Nov.-Dec. 1964, pp. 626–634.

[2] Staff Report. "Composite Engines," *Space/Aeronautics*, Vol. 48, No. 3, Aug. 1967, pp. 83–90.

[3] Peters, C. E., Peters, T., and Billings, R. B., "Mixing and Burning of Bounded Coaxial Streams," AEDC-TR-65-4, March 1965, Arnold Engineering Development Center; also available from Defense Documentation Center as AD458348.

[4] Cunningham, T. H. M. and Peters, C. E., "Further Experiments on Mixing and Burning of Bounded Coaxial Streams," AEDC-TR-68-136, Oct. 1968, Arnold Engineering Development Center; also available from Defense Documentation Center as AD676646.

[5] Peters, C. E., "Turbulent Mixing and Burning of Coaxial Streams Inside a Duct of Arbitrary Shape," AEDC-TR-68-270, Jan. 1969, Arnold Engineering Development Center; also available from Defense Documentation Center as AD680397.

[6] Fabri, J. and Paulon, J., "Théorie et Expérimentation des Ejecteurs Supersonique Air-Air," Note Technique 36, 1956, Office National d'Études et de Recherches Aérospatiales; English transl. TM 1410, Sept. 1958, NACA.

[7] Edelman, R. and Fortune, O., "An Analysis of Mixing and Combustion in Ducted Flows," AIAA Paper 68-114, New York, 1968.

[8] Edelman, R. and Weilerstein, G., "A Solution of the Inviscid-Viscid Equations with Application to Bounded and Unbounded Multicomponent Reacting Flows," AIAA Paper 69-83, New York, 1969.

[9] Chow, W. L. and Addy, A. L., "Interaction between Primary and Secondary Streams of Supersonic Ejector Systems and Their Performance Characteristics," *AIAA Journal*, Vol. 2, No. 4, April 1964, pp. 686–695.

[10] Chow, W. L. and Yeh, P. S., "Characteristics of Supersonic Ejector Systems with Nonconstant Area Shroud," *AIAA Journal*, Vol. 3, No. 3, March 1965, pp. 525–527.

[11] Libby, P. A., "Theoretical Analysis of Turbulent Mixing of Reactive Gases with Application to Supersonic Combustion of Hydrogen," *ARS Journal*, Vol. 32, No. 3, March 1962, pp. 388–396.

[12] Donaldson, C. duP. and Gray, K. E., "Theoretical and Experimental Investigation of the Compressible Free Mixing of Two Dissimilar Gases," *AIAA Journal*, Vol. 4, No. 11, Nov. 1966, pp. 2017–2025.